Electronic Supplementary Material (ESI) for Materials Chemistry Frontiers.

Mn dopant induced high-valence Ni^{3+} sites and oxygen vacancies for enhanced water oxidation

Yu Zhang,[a] Zhiyuan Zeng,* [a] and Derek Ho * [a]

[a] *Department of Materials Science and Engineering, City University of Hong Kong, 83 Tat Chee Avenue, Kowloon, Hong Kong 999077, China.*

E-mail: zhiyzeng@cityu.edu.hk; derekho@cityu.edu.hk

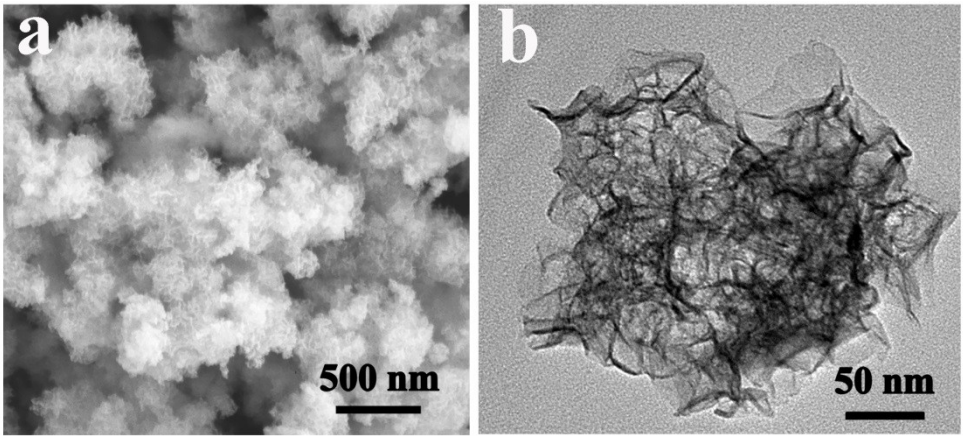

Fig. S1 (a) SEM and (b) TEM images of the Ni-Fe-O nanosheets.

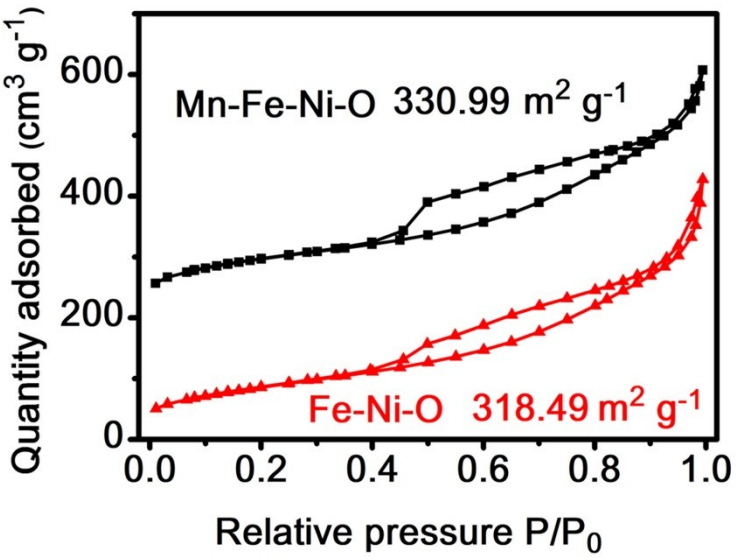

Fig. S2 N_2 adsorption-desorption curves of Ni-Fe-O and Mn-Ni-Fe-O nanosheets.

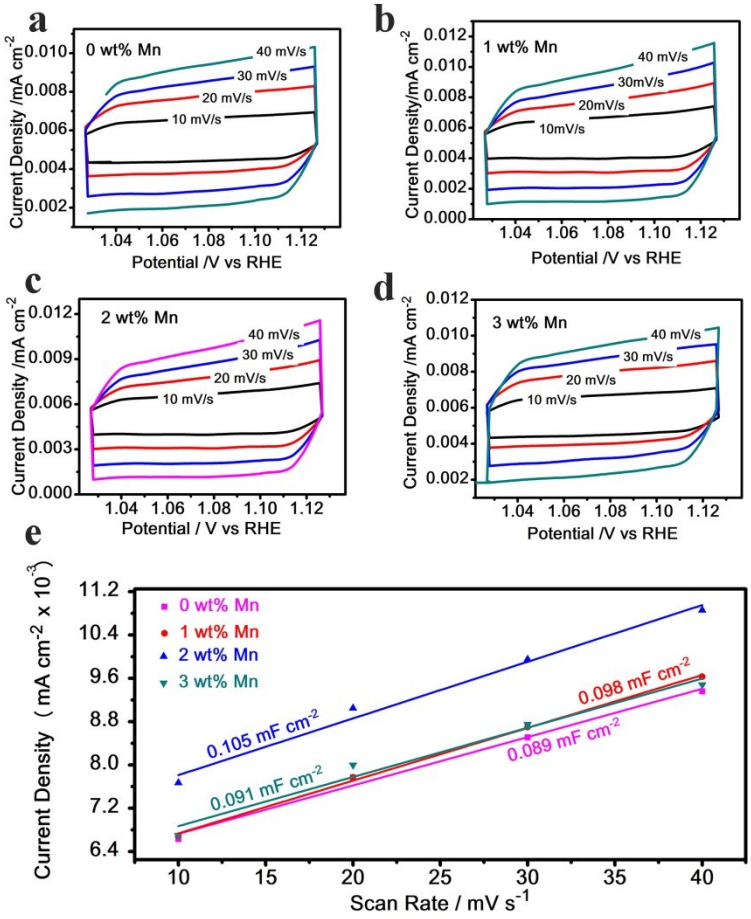

Fig. S3. Cyclic voltammetry (CV) curves of (a) pristine Ni-Fe-O nanosheets, (b) Mn-Ni-Fe-O nanosheets 1 wt% Mn dopant, (c) Mn-Ni-Fe-O nanosheets 2 wt% Mn dopant and (d) Mn-Ni-Fe-O nanosheets 3 wt% Mn dopant modified electrodes in the double layer region at scan rates of 10, 20, 30 and 40 mV s^{-1} in 1 M KOH. (e) Plots of the current density across scan rate for different Mn doping concentrations at 1.07 V vs RHE.

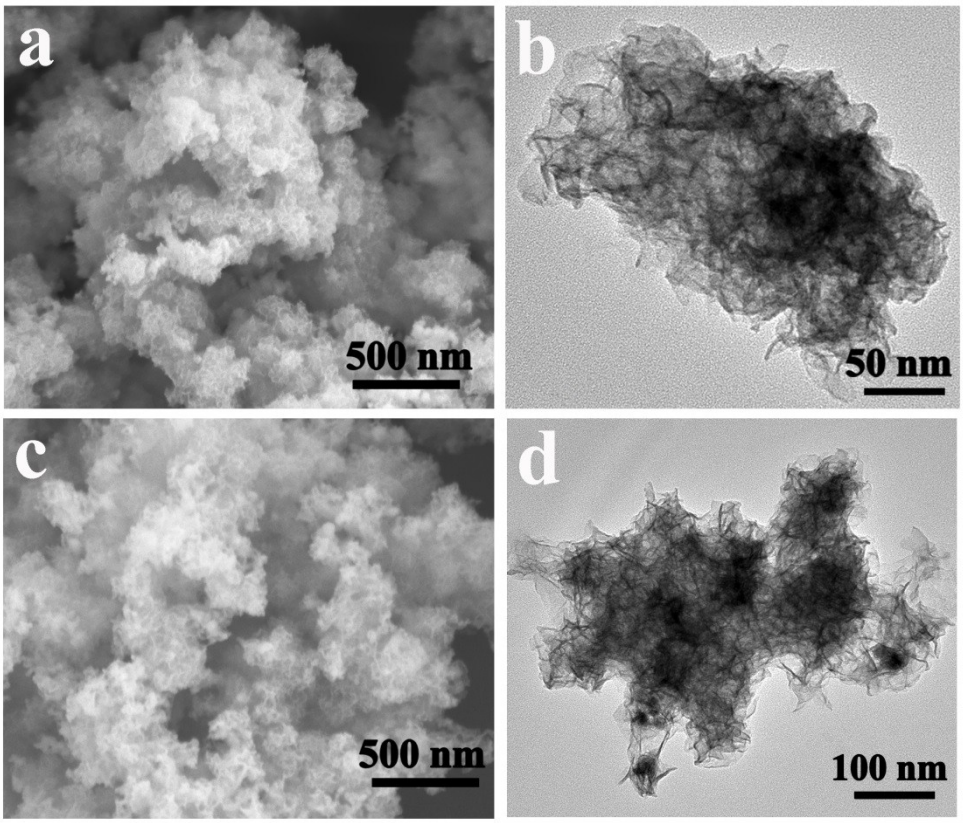

Fig. S4 (a) SEM and (b) TEM images of Mn-Ni-Fe-O nanosheets with 1 wt% Mn dopant; (c) SEM and (d) TEM images of Mn-Ni-Fe-O nanosheets with 3 wt% Mn dopant.

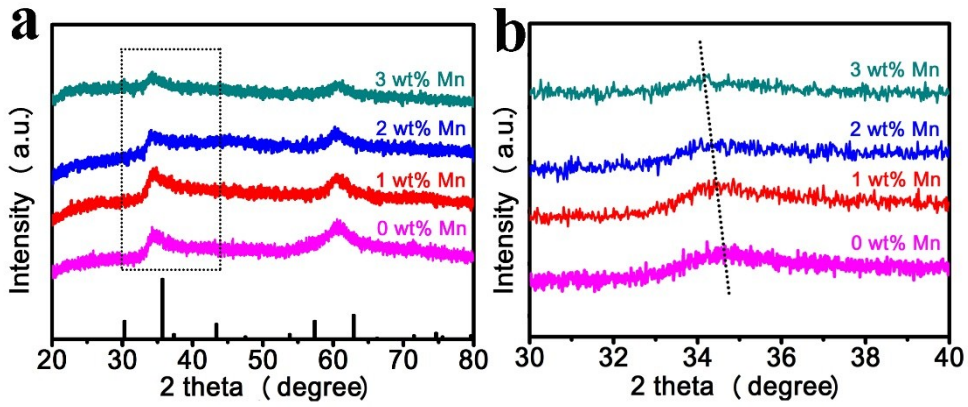

Fig. S5 (a) XRD pattern of Mn-Ni-Fe-O nanosheets across Mn doping concentrations, and (b) enlarged patterns of Fig. S5(a).

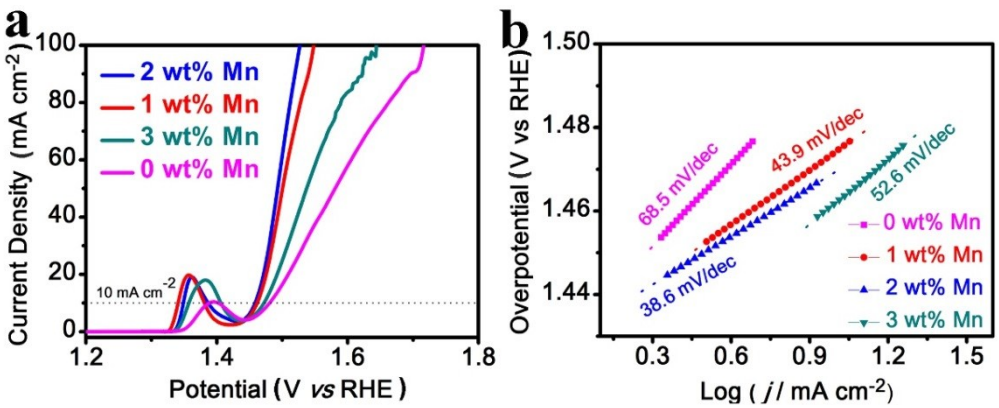

Fig. S6 (a) Polarization curves and (b) Tafel slope of Mn-Ni-Fe-O nanosheets across Mn doping concentrations.

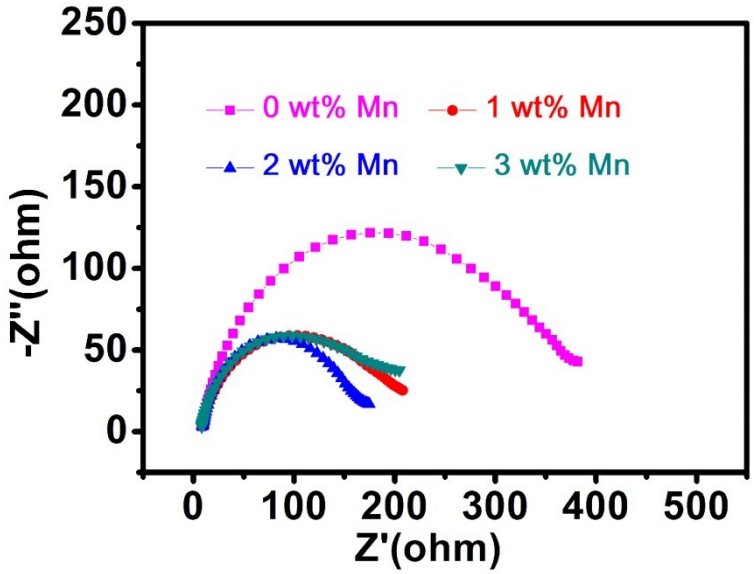

Fig. S7 Nyquist plots of Mn-Ni-Fe-O nanosheets across Mn doping concentrations.

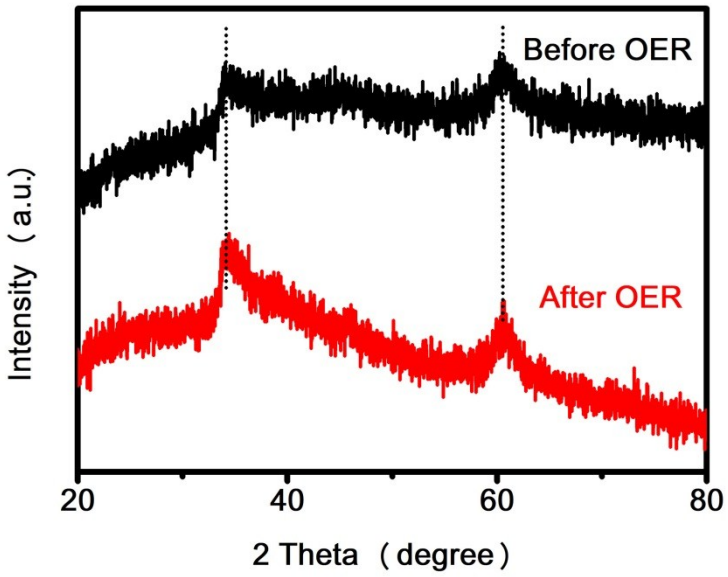

Fig. S8 XRD patterns of 2 wt% Mn-Ni-Fe-O nanosheets before and after 36 h OER stability test.

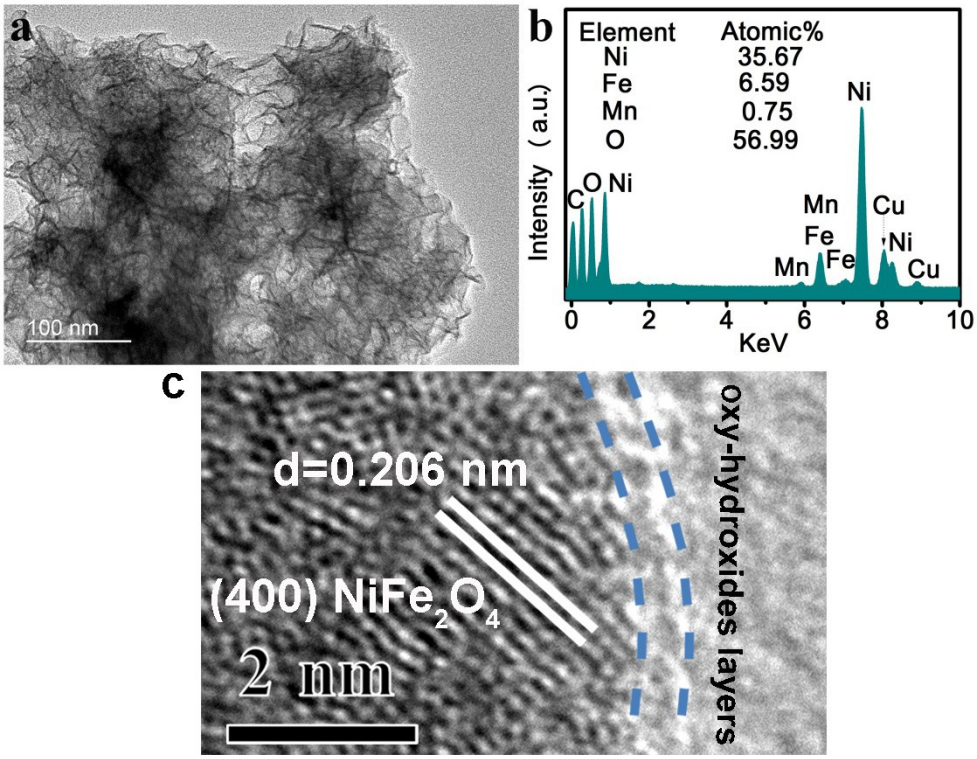

Fig. S9 (a) TEM image, (b) EDX spectrum, and (c) HRTEM image of 2 wt% Mn-Ni-Fe-O nanosheets after 36 h OER stability test.

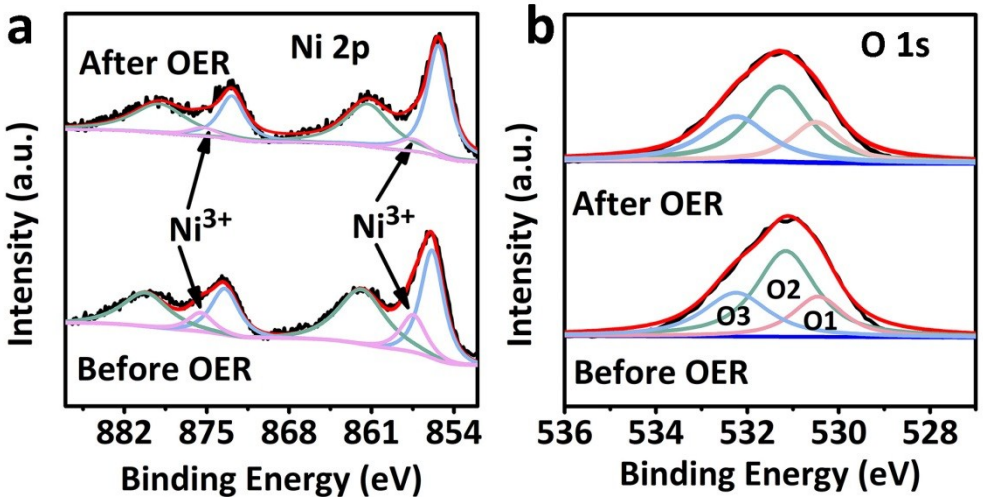

Fig. S10 XPS spectra of 2 wt% Mn-Ni-Fe-O nanosheets before and after OER after 36 h OER stability test: (a) Ni 2p and (b) O 1s.

Table S1. Mass ratios of Fe, Ni and Mn of the nanosheets obtained from ICP-OES.

Element Sample	Ni (wt%)	Fe (wt%)	Mn (wt%)
Ni-Fe-O nanosheets	39.2%	6.97%	0
Mn-Ni-Fe-O (1%) nanosheets	41.4%	6.02%	1.04%
Mn-Ni-Fe-O (2%) nanosheets	38.9%	6.45%	1.89%
Mn-Ni-Fe-O (3%) nanosheets	37.1%	6.07%	2.93%

Table S2. Comparison of OER catalytic parameters.

Catalyst	Substrate	η at J= 10 mA cm^{-2} (mV)	Tafel slope (mV dec^{-1})	Ref.
2 wt% Mn-Ni-Fe-O nanosheets	GC electrode	225 297 @η=100 mA cm^{-2}	38.2	This work
Ni-Fe-O nanosheets	GC electrode	250	68.5	This work
1 %wt Mn-Ni-Fe-O nanosheets	GC electrode	231	43.9	This work
3 %wt Mn-NiFe-O nanosheets	GC electrode	242	52.6	This work
$Ni(OH)_2$-NP	GC electrode	260	78.6	1
Porous NiO	GC electrode	310	54	2
$Fe(TCNQ)_2$/Fe	GC electrode	340	110	3
$Ni_{0.83}Fe_{0.17}(OH)_2$	GC electrode	245	61	4
NiFe LDHs-V_{Ni}	GC electrode	229	62.9	5
tannin-NiFe	Carbon fiber paper	290	28	6
Fe7.2%-Ni_3S_2 NSs/NF	Ni foam	320 (@η=20mA cm^{-2})	71	7
$Fe_{0.5}Mn_{0.5}OOH$	FTO	246	71	8
Fe–Mn–O NS/CC	Carbon cloth	273	63.9	9
NiMn LDH	GC electrode	330	47	10
NiO/MnO_2@PANI	GC electrode	345	42	11
Mn-NiFe-LDH/Ni foam	Ni foam	190	68	12
$FeNi_8Co_2$ LDH	Ni foam	210	42	13
NiFeV LDHs/Ni foam	Ni foam	192	39.2	14
NiCd(A)Fe	Polycrystalline titanium	290	38	15
(Fe, V, Co, and Ni) doped MnO_2	Carbon Fiber Paper	390	104.4	16
Co-MnO_2|O_V	GC electrode	279	75	17
CDs0.15-MnO_2	GC electrode	343	43.6	18
NF-Ni_3S_2/MnO_2	Ni foam	260	69	19

Notes: GC is glassy carbon; LDH is layered double hydroxides; PANI is polyaniline;

Table S3. The fitted results of the EIS plots in Fig. 4d and Fig. S7

Sample	R_{ct} (Ohm)
Ni-Fe-O nanosheets	347.8
Mn-Ni-Fe-O (1%) nanosheets	184.3
Mn-Ni-Fe-O (2%) nanosheets	155.7
Mn-Ni-Fe-O (3%) nanosheets	195.4

References：

1. C. Luan, G. Liu, Y. Liu, L. Yu, Y. Wang, Y. Xiao, H. Qiao, X. Dai, and X. Zhang, ACS Nano 2018, 12, 4, 3875-3885.
2. P. T. Babar, A. C. Lokhande, M. G. Gang, B. S. Pawar, S. M. Pawar, and J. Hyeok Kim. J. Ind. Eng. Chem., 2018, 60, 493–497.
3. M. Xie, X. Xiong, L. Yang, X. Shi, A. M. Asiri and X. Sun, Chem. Commun., 2018, **54**, 2300-2303.
4. Q. Zhou, Y. Chen, G. Zhao, Y. Lin, Z. Yu, X. Xu, X. Wang, H. K. Liu, W. Sun and S. X. Dou, ACS Catal., 2018, 8, 5382-5390.
5. Y. Wang, M. Qiao, Y. Li and S. Wang, Small, 2018, 14, 1800136-1800141.
6. Y. Shi, Y. Yu, Y. Liang, Y. Du and B. Zhang, Angew. Chem. Int. Ed., 2019, **58**, 3769-3773.
7. Y. Zhu, H. Yang, K. Lan, K. Iqbal, Y. Liu, P. Ma, Z. Zhao, S. Luo, Y. Luo and J. Ma, Nanoscale, 2019, 11, 2355-2365
8. M. P. Suryawanshi, U. V. Ghorpade, S. W. Shin, U. P. Suryawanshi, H. J. Shim, S. H. Kang, and J. H. Kim, Small, 2018, 14, 1801226-1801233.
9. Y. Teng, X. Wang, J. Liao, W. Li, H. Chen, Y. Dong, and D. Kuang, Adv. Funct. Mater. 2018, 28, 1802463-1802470.
10. R. Li, Y. Liu, H. Li, M. Zhang, Y. Lu, L. Zhang, J. Xiao, F. Boehm and K. Yan, Small Methods, 2019, 3, 1800344-1800348.
11. J. He, M. Wang, W. Wang, R. Miao, W. Zhong, S. Chen, S. Poges, T. Jafari, W. Song, J. Liu, and S.-L. Suib, ACS Appl. Mater. Inter., 2017, 9, 42676−42687.
12. D. Zhou, Z. Cai, Y. Jia, X. Xiong, Q. Xie, S. Wang, Y. Zhang, W. Liu, H. Duan and X. Sun, Nanoscale Horiz., 2018, 3, 532-537.
13. X. Long, S. Xiao, Z. Wang, X. Zheng and S. Yang, Chem. Commun., 2015, 51, 1120-1123.
14. P. Li, X. Duan, Y Kuang, Y. Li, G. Zhang, W. Liu and X. Sun, Adv. Energy Mater, 2018, 8, 1703341-1703347.
15. J.-H. Kim, D. H. Youn, K. Kawashima, J. Lin, H. Lim and C. B. Mullins, Appl. Catal. B: Environ., 2018, 225, 1-7.
16. Z. Ye, T. Li, G. Ma, Y. Dong, and X. Zhou, Adv. Funct. Mater. 2017, 27, 1704083-1704090.
17. Y. Zhao, J. Zhang, W. Wu, X. Guo, P. Xiong, H. Liu, G. Wang, Nano Energy, 2018, 54, 129-137.
18. L. Tian, J. Wang, K. Wang, H. Wo, X. Wang, W. Zhuang, T. Li, X. Du, Carbon, 143, 2019, 457-466.

19. Y. Xiong, L. Xu, C. Jin, Q. Sun, Appl. Catal. B: Environ., 2019, 245, 329-338.